HBRP PUBLICATION

Research and Reviews: Journal of Mechanics and Machines
Volume 4 Issue 1

Computational Fluid Dynamics Analysis on Turbulent Kinetic Energy Distribution of NACA 0018 Airfoil at Two Reynolds Number

***Md. Abdus Shabur*[1*], *Md. Asif Hasan Khan*[2], *Nafis Saad Resan*[3]**
[1]*Lecturer,* [2]*Assistant Engineer,* [3]*Student*
[1]*Department of Mechatronics and Industrial Engineering, Chittagong University of Engineering and Technology, Chattogram-4349, Bangladesh*
[2]*Jalalabad Gas Transmission & Distribution System Ltd., Bangladesh*
[3]*Department of Mechanical Engineering, Chittagong University of Engineering and Technology, Chattogram-4349, Bangladesh*

***Corresponding Author**
***E-mail Id*:-** *abdusshabur@cuet.ac.bd*

ABSTRACT

The aerodynamic attributes of an airfoil must be evaluated both computationally and experimentally in order to improve its design and performance. The turbulence kinetic energy of a symmetric airfoils NACA 0018 was investigated in this study for two separate low Reynolds numbers of 300,000 and 700,000. This computational simulation work, which was carried out using the Ansys FLUENT 14.5 software, yields some interesting results. The distribution of turbulence kinetic energy across airfoil surfaces at various angles of attack and under two different airstream velocities is illustrated in this paper. Due to flow separation, there has been a big amount of turbulence observed after the stall angle [2]. The final results show that the NACA 0018 airfoil produces significant turbulence as the thickness of the airfoil increases, there is more friction with the air particle. In the second comparison, in terms of Reynolds number or airstream velocity, higher velocity produces more turbulence, as shown by the red zone in the figures. As turbulence is always expected to be as low as possible in aircraft [14], therefore, it is recommended not to use NACA 0018 airfoil in aircraft applications and rather it can be l in vertical axis wind turbine or horizontal axis wind turbine applications where turbulence is of less importance.

Keywords:-*Airfoil, Reynolds Number, Turbulence Kinetic Energy, NACA, Angle of Attack*

INTRODUCTION

Any airfoil's aerodynamic properties must be investigated, that's why a large number of aerodynamic parameters must be investigated experimentally and numerically to achieve the desired performance of the airfoil. The cross sectional form of a wing, blade (of a propeller, turbine, or rotor), or sail is referred to as an airfoil.

Aerodynamic force is created when an airfoil-shaped body passes through a fluid [6]. The lift component is the component of this force that is perpendicular to the direction of motion. The component of motion that is perpendicular to the direction of motion is called drag. Subsonic flight airfoils have a characteristic form, with a rounded leading edge and a sharp following edge, and symmetrical curvature of the upper and lower surfaces Hydrofoils are foils with comparable functions that use water as the working fluid.

In Computational Fluid Dynamics (CFD) analysis, the coefficients of lift (C_L), drag

(C_D), and the variation of the C_L/ C_D ratio, as well as the turbulence kinetic energy distribution with angle of attack, are all critical factors [7]. To calculate these symmetric and asymmetric airfoil features, many modeling approaches such as Standard k-, RNG k-, SST k-, and others are extensively employed. This work investigates the aforementioned characteristics, as well as turbulent kinetic energy, for symmetric airfoils NACA0018 at low Reynolds numbers of 300,000 and 700,000 [4]. NACA is an acronym for the National Advisory Committee for Aeronautics [17] In In fluid dynamics, turbulence kinetic energy (TKE) is the mean kinetic energy per unit mass associated with eddies in turbulent flow. Turbulence's kinetic energy is defined by observed root-mean-square (RMS) velocity variations. The turbulence kinetic energy may be calculated in the Reynolds-averaged Navier-Stokes equations using the closure technique, i.e. a turbulence model. TKE is often computed as half of the sum of the variances (square of standard deviations) of the velocity components.$k = \frac{1}{2}\left(\left(\overline{(u')^2}\right) + \left(\overline{(v')^2}\right) + \left(\overline{(w')^2}\right)\right)$

where the turbulent velocity component is defined as the difference between the instantaneous and average velocity $u' = u - u'$, whose mean and variance are

$$\bar{u'} = \frac{1}{T}\int_0^T (u(t) - u')dt = 0$$

and

$$\overline{(u')^2} = \frac{1}{T}\int_0^T (u(t) - u')^2 dt = 0$$

respectively [16].

An open-source commercial CFD code, FLUENT (version 14.5), is used in this research. [13]. In order to calculate the fluctuation of C_L and C_D with angle of attack, the SST k-turbulence model is employed [5]. This numerical simulation has been validated with a previously conducted experimental inquiry.

.

LITERATURE REVIEW

Timmer [9] tested the balance and wake rake of a 0.25 m chord model with a NACA 0018 airfoil in the Delft University low-turbulence wind tunnel. According to the test results, the lower surface laminar separation bubble dominates the flow and noise characteristics at Reynolds numbers between 150000 and 1000000. This study included experimental data for C_D vs. angle of attack and C_L vs. angle of attack.

During a large variety of Reynold number which extends into the flying area, Jacobs and Sherman [8] examined symmetric airfoils in the NACA variable-density wind tunnel. The tests were carried out to offer information from which changes in the Reynolds number might be derived from variations in the airfoil section and methods for allowing these variations in practice.

In the TsAGI's T-124 low-turbulence wind tunnel, Sereez et al. [2] explored aerodynamic static hysteresis for the NACA0018 airfoil at stall circumstances. Experimental wind tunnel data for 2D NACA0018 and NACA0012 airfoils with low Reynolds numbers (Re =300,000) were evaluated to the findings of computer models. When comparing static testing and slow sweep variations in angle of

attack, the researchers discovered that the breadth of the static hysteresis loop differed. This finding suggests that abrupt transitions between distinct separated flow topologies are more sensitive.

MR Ahmed et al. [5] studied a low Reynolds number airfoil for wind turbine blades. They found that higher angles of attack delayed separation from the upper surface, increasing lift and reducing drag. The lift-to-drag ratio increased by 8% to 15% as turbulence increased in the angles of attack-range of interest.

NUMERCAL APPROACH

Basics of CFD

In philosophical research and the growth of the entire field of fluid dynamics, the computer fluid dynamic is a relatively recent technique. High-speed digital computing innovation in conjunction with the development of accurate numerical algorithms for physical problem solving on these computers has transformed how fluid dynamics are used today. Computational fluid dynamics is today an equal partner in the analysis and resolution of fluid dynamics problems alongside theory and pure experiment. Applying the basic mechanical rules to a fluid produces the equations for a fluid [1].

Governing Equation

The computation has been carried out with the help of some fundamental fluid dynamics formulas [12].

The conservation of mass equation is in vector form

$$\frac{\partial \rho}{\partial t} + \nabla.(\rho V) = 0 \qquad (1)$$

And the conservation of momentum equation is

$$\rho \frac{\partial V}{\partial t} + \rho\big((V.)V\big)V == -\nabla\rho + \rho g \ + \nabla.\tau \qquad (2)$$

Where, ∇ is the velocity vector.

Assuming that the density of the flow is constant and that the continuity equation (conservation of mass) and the Navier-Stokes equation (conservation of momentum) are valid, the following equations govern the current investigation:

1. Conservation of mass

$$\frac{1}{\rho}\frac{\partial \rho}{\partial t} + \frac{\partial(u)}{\partial x} + \frac{\partial(v)}{\partial y} + \frac{\partial(w)}{\partial z} = 0 \quad ; For\ 3D\ flow \quad \ldots\ldots\ldots\ldots(3)$$

$$\frac{1}{\rho}\frac{\partial \rho}{\partial t} + \frac{\partial(u)}{\partial x} + \frac{\partial(v)}{\partial y} = 0 \quad ; For\ 2D\ flow \quad \ldots\ldots\ldots\ldots\ldots (4)$$

Conservation of momentum

For 3-D flow,

$$\rho\left(\frac{\partial(u)}{\partial t} + u\frac{\partial(u)}{\partial x} + v\frac{\partial(u)}{\partial y} + w\frac{\partial(u)}{\partial z}\right) + \frac{\partial(\rho)}{\partial x} = \mu\left(\frac{\partial^2(u)}{\partial x^2} + \frac{\partial^2(u)}{\partial y^2} + \frac{\partial^2(u)}{\partial z^2}\right) \ldots\ldots\ldots\ldots\ldots(5)$$

$$\rho\left(\frac{\partial(v)}{\partial t}+u\frac{\partial(v)}{\partial x}+v\frac{\partial(v)}{\partial y}+w\frac{\partial(v)}{\partial z}\right)+\frac{\partial(\rho)}{\partial y}$$
$$=\mu\left(\frac{\partial^2(v)}{\partial x^2}+\frac{\partial^2(v)}{\partial y^2}+\frac{\partial^2(v)}{\partial z^2}\right)\ldots\ldots\ldots\ldots\ldots(6)$$
$$\rho\left(\frac{\partial(w)}{\partial t}+u\frac{\partial(w)}{\partial x}+v\frac{\partial(w)}{\partial y}+w\frac{\partial(w)}{\partial z}\right)+\frac{\partial(\rho)}{\partial z}$$
$$=\mu\left(\frac{\partial^2(w)}{\partial x^2}+\frac{\partial^2(w)}{\partial y^2}+\frac{\partial^2(w)}{\partial z^2}\right)\ldots\ldots\ldots\ldots\ldots(7)$$

Assuming that molecular viscosity is constant, and making the Bussines approximation, the TKE equation is:

$$\frac{\partial k}{\partial t}+\bar{u}_j\frac{\partial k}{\partial x_j}=-\frac{1}{\rho_o}\frac{\partial\overline{u'_\iota p'}}{\partial x_i}-\frac{1}{2}\frac{\partial k\overline{u'_J u'_J u'_\iota}}{\partial x_i}+\upsilon\frac{\partial^2 k}{\partial x_i{}^2}-\overline{u'_\iota u'_J}\frac{\partial\overline{u'_\iota}}{\partial x_j}-\upsilon\frac{\overline{\partial u'_\iota}}{\partial x_J}\frac{\partial u'_\iota}{\partial x_J}\frac{\partial\overline{u'_\iota p'}}{\partial x_i}-$$
$$\frac{g}{\rho_o}\overline{\rho' u'_\iota}\delta_{i3}\ldots\ldots\ldots\ldots\ldots(8)$$

GEOMETRY

The airfoil employed in this investigation is shown in Figure 1 and Figure 2. For both airfoils, the chord length is 1m. The radius of the mesh's 'C' is 12.5 meters. For NACA0018 the maximum chord length is 18%.

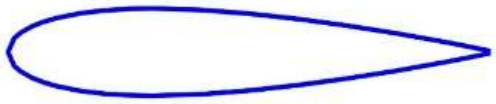

Fig.2:-*NACA 0018 airfoil*

Meshing

For a high-quality CFD analysis, the grid system is crucial. In this work, a 2D unstructured mesh with a total number of cells of around 89000 is used in both airfoils. The maximum and minimum face areas for the NACA 0018 airfoil are 3.360926 m2 and 1.896361x10-4 m2, respectively.

Figure 3 depicts the meshing domain. Figure 4 shows zoomed-in images of the meshing around the airfoil surface.

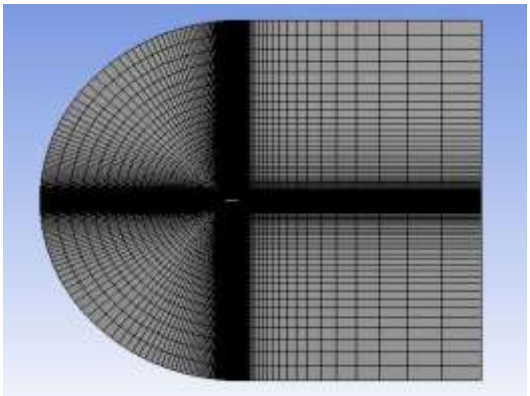

Fig.3:-*Meshing domain for NACA 0018 airfoil*

Fig.4:-*Magnified view of meshing for NACA0018 airfoil*

Solver Setting [Table 1]

Ansys FLUENT 14.5 is used for the calculations. C_L and C_D fluctuation with angle are calculated using the SST k-turbulence model. The governing integral equations for mass and momentum conservation were solved using this CFD program.

Table 1:-*Solver Setting*

Solver	Velocity formulation	2D Space	Time
Pressure based	Absolute	Planer	Steady

Boundary Conditions

Inlet: The boundary condition for the velocity inlet is employed. The inlet velocity for Re=300,000 was 4.38 m/s, whereas the inlet velocity for Re=700,000 was 10.23 m/s.

Outlet: The boundary condition of the pressure outlet is used. The gauge pressure at the outlet border is kept constant at 0 Pa.

Wall: A stationary wall with the no-slip condition has been employed at all solid boundaries in the flow geometry. It can be stated mathematically as u_{wall}=0 m/s.

Solution Method

Coupled technique was employed for pressure-velocity coupling in this investigation. In numerous ways, this solver outperforms the pressure-based segregated method. For steady-state flows, the pressure-based coupled technique yields a more resilient and economical single phase implementation. The gradient was derived using least squares cells in the spatial discretization, the pressure was second order, the momentum was second order upwind, and the turbulent kinetic energy and specific dissipation rate were first order upwind. The Courant-Friedrichs-Lewy (CFL) number remained constant at 0.9, as did the pressure and momentum explicit relaxation factors, both of which were 0.75.

RESULTS AND DISCUSSION

Validation[Table 2]

Here two experimental investigations were used for validation in this case. Timmer [9] in 2008 and Jacobs [8] in 1937 are two examples. Computed results of this study were substantially identical to the experimental data. This simulation results were validated for the NACA0018 airfoil at Re=300000 and Re=700000. The graphical validation findings are provided below:

Table 2:- *Comparison of our model's C_L and C_D with the experimental results for NACA 0018 at Re = 300,000 [7]*

Value of C_D			
AOA	Our Study	Jacob	Timmer
5°	0.017397	0.024	.023
10°	0.025715	0.028	0.027
15°	0.051888	0.04	0.06

Value of C_L			
AOA	Our Study	Jacob	Timmer
5°	0.43726	0.48	0.47
10°	0.85221	0.85	0.93
15°	1.2207	1.00	1.04

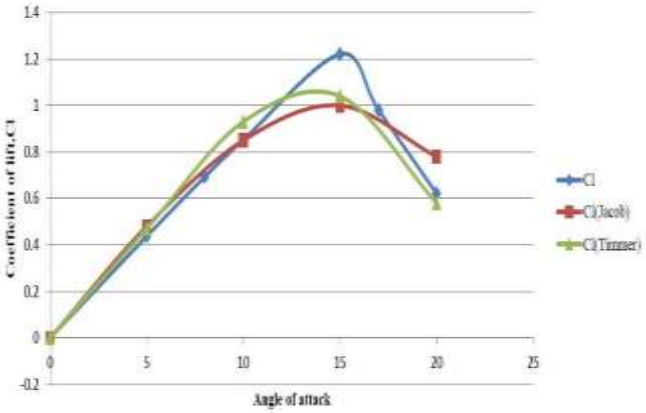

Fig.5:-*Comparison of our models' calculated coefficient of lift (C_L) and the experimental data for NACA 0018 at Re = 300,000*

Figure 5 makes it obvious that the C_L is proportionate to the angle of attack up to the angle of stall (almost 16 degrees), then quickly drops beyond that angle. It is because the air stream is back flowing [7].

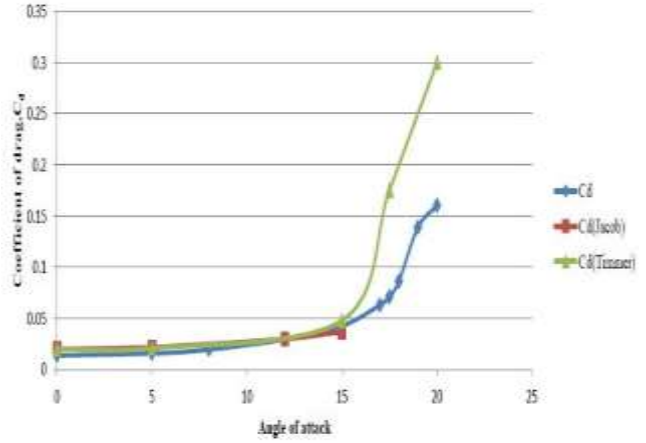

Fig.6:-*Comparison of our models' calculated coefficient of drag (C_D) and the experimental data for NACA 0018 at Re = 700,000*

Based on these graphs, we can conclude that our simulation work is correct and up to the mark. Our researched data almost matches the experimental data up to the stall angle, but after the stall angle, the features are unknown as shown in Figure 6.

RESULTS

Turbulent Kinetic Energy Distribution for NACA 0018 at Re=300,000

At first, turbulent kinetic energy distribution has been shown for NACA 0018 airfoil. The color gradient depicted in the figures below indicates the value of the turbulent kinetic energy distribution across the airfoil. The blue color denotes the smallest value, while the red color denotes the greatest value. The turbulent kinetic energy distribution as shown in Figure 7-10 reveals that at zero incidence, it is concentrated in a small area near the trailing edge, but as the angle of attack increases, the value of the turbulent kinetic energy increases near the trailing edge and spreads across the upper surface of the airfoil. As a result, we can conclude that the TKE distribution characteristics follow a similar pattern up to the stall angle of attack, which is approximately 17 degrees

as shown in Figure 11.

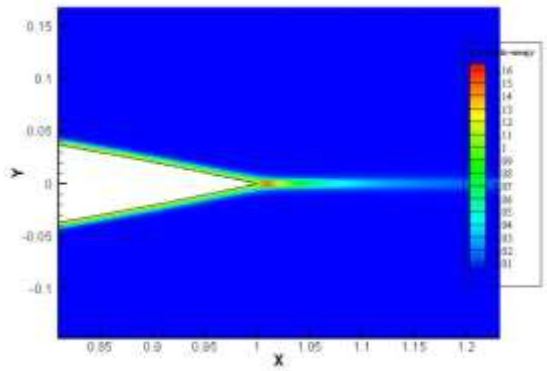

Fig.7:-*Turbulent Kinetic Energy at 0 degree AOA*

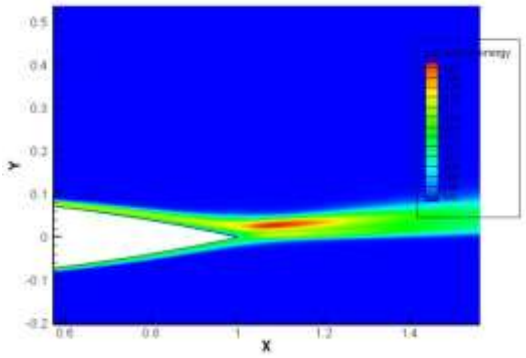

Fig.8:-*Turbulent Kinetic Energy at 5 degree AOA*

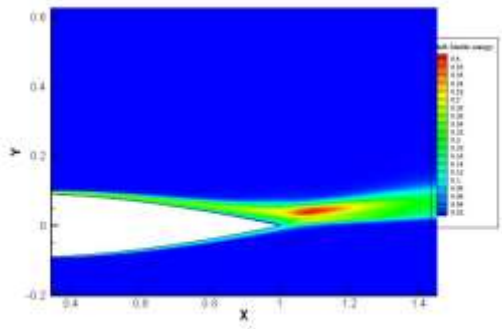

Fig.9:-*Turbulent Kinetic Energy at 8 degree AOA*

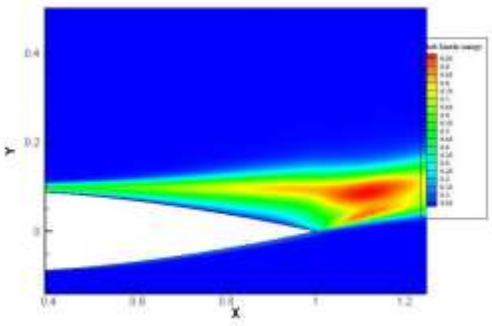

Fig.10:-*Turbulent Kinetic Energy at 15 degree AOA*

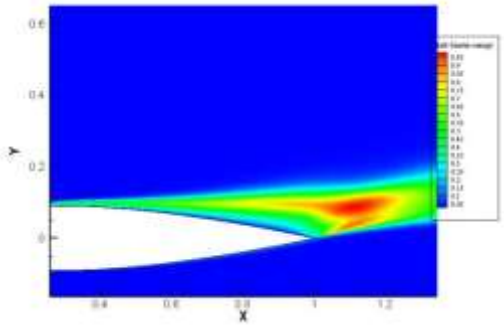

Fig.11:*-Turbulent Kinetic Energy at 17 degree AOA*

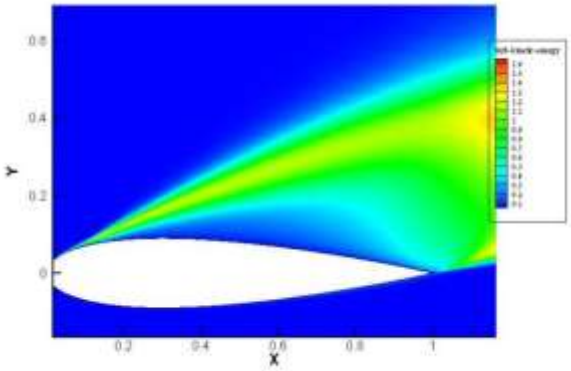

Fig.12:*-Turbulent Kinetic Energy at 20 degree AOA*

For a 20 degree angle of attack, as illustrated in Figure 12, there is a wake region above the upper surface of the airfoil with a very low value, but a higher value above this region. This is due to the turbulence generated as a result of the flow separation. Due to the fact that the attack angle here (20 degrees) is greater than the stall angle (16 degrees), the pattern of TKE distribution changes significantly, as in previous cases. However, unlike in previous cases, the red zone is less prominent in this one. A large area of somewhat reddish green dominates.

Turbulent Kinetic Energy Distribution for NACA 0018 at Re=700,000

To observe the variation with the previous case, the Reynolds number has been increased to 700,000 in this case. As a result, the Figures 13-18 below show a significant change. As the Reynolds number rises, so does the corresponding air velocity. As a result, turbulence increases to some extent. The TKE distribution characteristics, like the previous Reynolds number, follow a similar pattern up to the stall angle of attack, which is adjacent to 17 degrees.

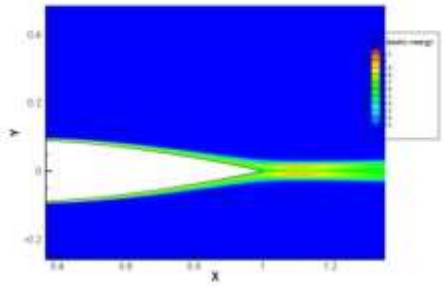

Fig.13:*-Turbulent Kinetic Energy at 0 degree AOA*

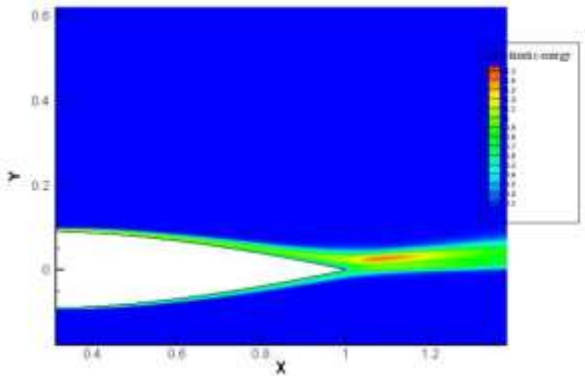

Fig.14:-*Turbulent Kinetic Energy at 5 degree AOA*

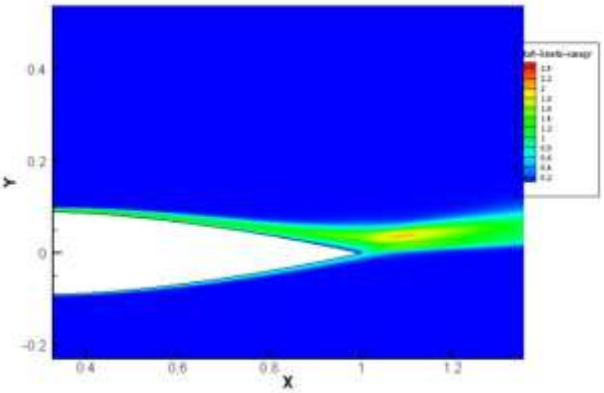

Fig.15:-*Turbulent Kinetic Energy at 8 degree AOA*

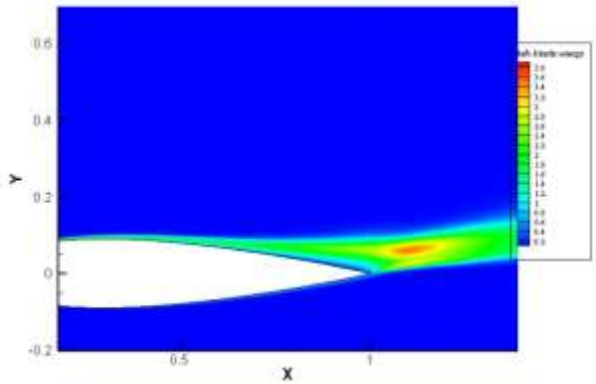

Fig.16:-*Turbulent Kinetic Energy at 12 degree AOA*

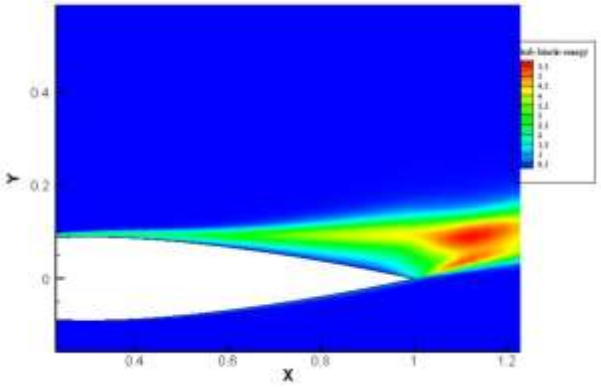

Fig.17:-*Turbulent Kinetic Energy at 15 degree AOA*

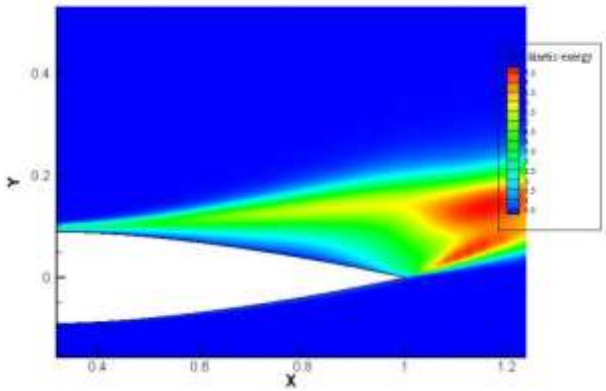

Fig.18:*-Turbulent Kinetic Energy at 17 degree AOA*

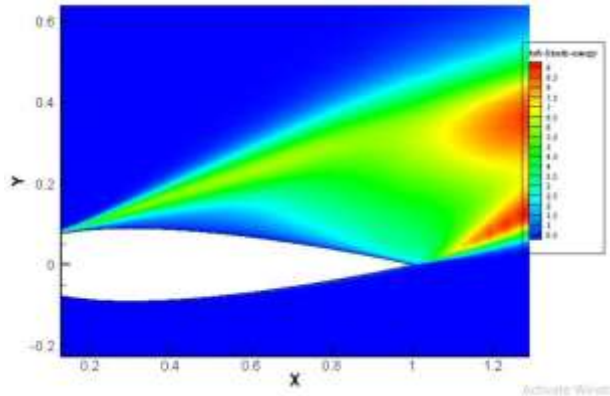

Fig.19:*-Turbulent Kinetic Energy at 20 degree AOA*

Unlike the previous case of Re=300,000, the red zone area increases in this case of a 20 degree angle of attack, as illustrated in Figure 19. This demonstrates that turbulence increases in direct proportion to the Reynolds number, or airstream velocity.

CONCLUSION

An analysis of turbulent kinetic energy distribution across two symmetric airfoils of different thickness at two distinct Reynolds numbers was demonstrated in this study using CFD simulation with Ansys FLUENT. Some interesting findings can be drawn here. The above figures show that the NACA 0018 airfoil produces significant turbulence. And it happens because as the thickness of the airfoil increases, there is more friction with the air particle. In the second comparison, in terms of Reynolds number or airstream velocity, higher velocity produces more turbulence, as shown by the red zone in the figures above. In aircraft applications, turbulence is always expected to be as low as possible [14]. Therefore, it is recommended not to use NACA 0018 airfoil in aircraft applications and rather it can be in vertical axis wind turbine or horizontal axis wind turbine applications where turbulence is of less importance.

ACKNOWLEDGEMENT

We would first of all like to thank Allah Almighty for giving us the strength to finish our work. In addition, we want to express our sincere appreciation for the valuable guidance and suggestion of all the teachers in the Department of Mechanical Engineering at BUET. This task would not have been possible to complete successfully without their initiative ideas, talents, guidelines and encouragements.

NOMENCLATURE

Symbol	Meaning	Unit
α	Angle of attack	(K)
P	Pressure	(Pa)
c	Chord length	(m)
x	Any distance from leading edge	(m)
u	X-component velocity	(m/s)
v	Y-component velocity	(m/s)
w	Z-component velocity	(m/s)
V_∞	Free-stream velocity	(m/s)
τ	Shear stress	(N/m^2)
μ	Viscosity	(Pa-s)
ρ	Density	(kg/m^3)
Re	Reynolds number ($\rho V_\infty L/ \mu$)	Dimension Less
t	Time	(s)
C_L	Coefficient of lift	Dimension Less
C_D	Coefficient of drag	Dimension Less

REFERENCES

1. Hassan, G. E., Hassan, A., & Youssef, M. E.(2015). Numerical investigation of medium range re numbers aerodynamics characteristics for NACA0018 airfoil. *CFD letters, 6*(4), 175-187.
2. Hoffmann, J. A., (1991). Effect of Freestream Turbulence on the Performance Characteristics of an Airfoil. *AIAA Journal, 29:* 1353-1356.
3. Sereez, M., Abramov, N., & Goman, M. (2016, July). Computational Simulation of Airfoils Stall Aerodynamics at Low Reynolds Numbers. *Royal Aeronautical Society, Applied Aerodynamics Conference.*
4. Ladson, C. L. (1988). Effects of independent variation of Mach and Reynolds numbers on the low-speed aerodynamic characteristics of the NACA 0012 airfoil section.
5. Ahmed, M. Rafiuddin & Narayan, Sumesh & Zullah, Asid & Lee, Young-Ho. (2011). Experimental and Numerical Studies on a Low Reynolds Number Airfoil for Wind Turbine Blades. *Journal of Fluid Science and Technology. 6*. 357-371. 10.1299/jfst.6.357.
6. Abbott, I. H., & Von Doenhoff, A. E. (1959). Theory of wing sections, including a summary of airfoil data. Courier Corporation.
7. Abdus Shabur, Afnan Hasan, & Mohammad Ali. (2020). Comparison of Aerodynamic Behaviour between NACA 0018 and NACA 0012 Airfoils at Low Reynolds Number Through CFD Analysis. *Advancement in Mechanical Engineering and Technology, 3*(2), 1–8.
8. Jacobs, E. N., & Sherman, A. (1937). Airfoil section characteristics as affected by variations of the Reynolds number.
9. Timmer, W. A. (2008). Two-dimensional low-Reynolds number wind tunnel results for airfoil NACA 0018. *Wind engineering, 32*(6),

525-537.
10. Brendel, M., & Mueller, T. J. (1988). Boundary-layer measurements on an airfoil at low Reynolds numbers. *Journal of aircraft, 25(*7), 612-617.
11. Hu, H., Yang, Z., & Igarashi, H. (2007). Aerodynamic hysteresis of a low-Reynolds-number airfoil. *Journal of Aircraft, 44*(6), 2083-2086.
12. Anderson Jr, J. D. (2010). Fundamentals of aerodynamics. *Tata McGraw-Hill Education*.
13. Release, A. N. S. Y. S. (2012). 14.5, User Guide. ANSYS, Inc.
14. https://www.aviationnepal.com/what-is-turbulence-can-turbulence-crash-a-plane-myths-of-turbulence/ (Date of access: 27/08/2021)
15. http://www.naca.com (Date of access: 27/08/2021)
16. https://en.wikipedia.org/wiki/Turbulence_kinetic_energy#cite_note-2 (Date of access: 15/08/2021)